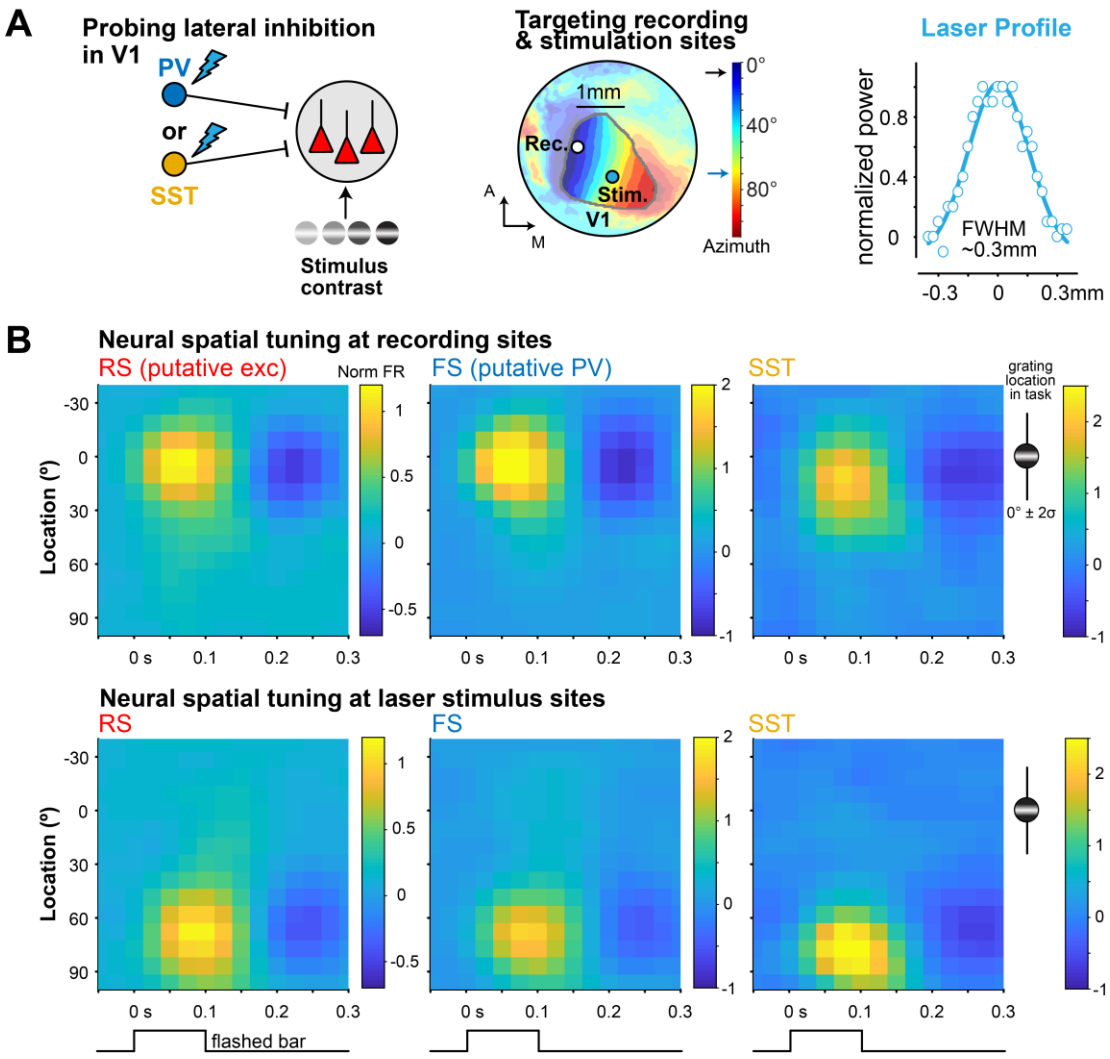

Figure S1. Precise targeting of retinotopic sites in V1.

A. Left, illustration of experimental paradigm to record from a retinotopic site in V1 while distally activating PV or SST neurons at another retinotopic site. Middle, example ISI map showing targeted recording and stimulation sites corresponding to different visual retinotopic locations in V1 (same as Fig. 1). Right, the laser beam profile size was small (0.334 mm full-width half-max) allowing precise stimulation of specific retinotopic sites.

B. The receptive fields of all neurons (1612 RS; 354 FS; 50 SST) were mapped by flashing bars (9˚ width, 0.1 s duration, 0.3 s inter-stimulus-interval) across multiple azimuth positions in the visual field (y-axis). Top, neurons in the targeted recording site in V1 had receptive fields at 10.2 ± 25.4˚ (peak ± σ), that largely overlapped with the task-relevant visual stimuli (Gabor Grating centered at 0˚, σ = ~10˚). Bottom, neurons in the targeted laser stimulation site had receptive fields at 73.4 ± 25.6˚ and were not activated by and did not overlap with the task-relevant visual stimuli. Z-scored firing rate activity plotted.

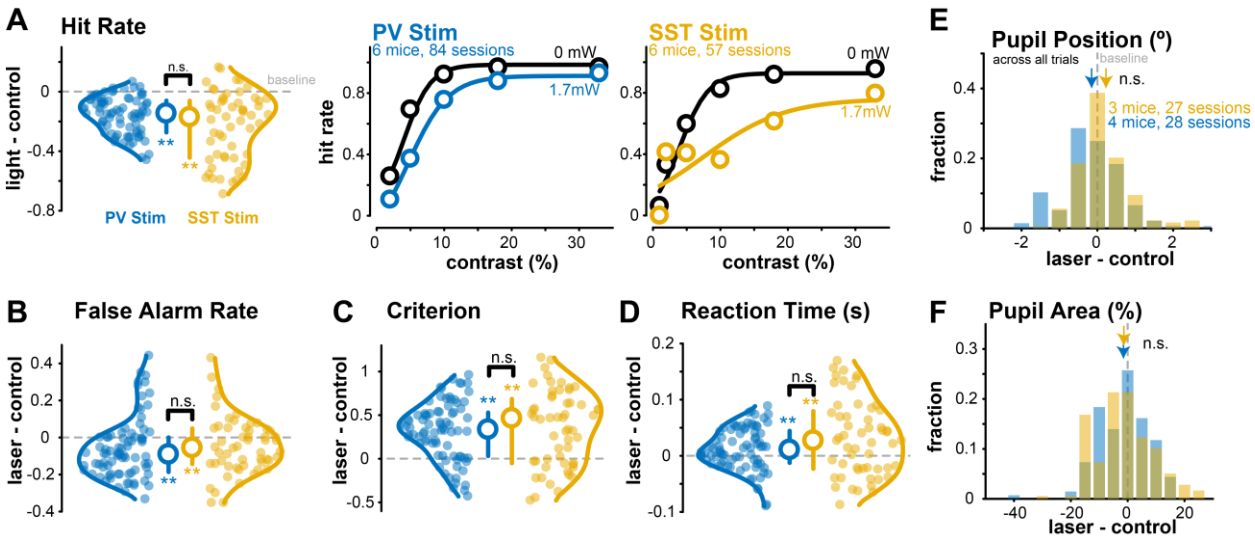

Figure S2. Behavioral metrics, pupil area, pupil position in PV and SST mice

A. Left, hit rate changes with distal PV stimulation (6 mice, 84 sessions) and distal SST stimulation (6 mice, 57 sessions), averaged over all contrasts (1 – 33%, Median ± IQR plotted). The hit rate decreases for both distal PV stimulation (Δ (laser – control) = –0.15 ± 0.11, median ± MAD, $p < 1e{-}12$, Wilcoxon signed-rank test) and distal SST stimulation (Δ (laser – control) = –0.17 ± 0.21, $p < 1e{-}7$). The overall magnitude of decrease in hit rate is not significantly different with distal PV vs SST stimulation ($p = 0.07$, Wilcoxon rank-sum test). Middle, hit rate sorted by contrasts in PV-ChR2 mice during control (0 mW) and distal PV stimulation sessions. Right, hit rate across contrasts for SST-ChR2 mice (6 mice, 57 sessions). Mean ± SEM, sigmoidal fits plotted. Distal SST stimulation decreases the hit rate slope (Δ (laser – control) = –0.06 ± 0.24, median ± MAD, $p = 0.04$), while PV stimulation slightly increases the slope (Δ = 0.03 ± 0.17, $p = 0.02$).

B. The false alarm rate decreases with distal SST stimulation (Δ = –0.06 ± 0.12, $p < 0.01$) and distal PV stimulation (Δ = –0.09 ± 0.13, $p < 1e{-}3$) and is not significantly different across groups ($p = 0.16$).

C. The criterion (likelihood to withhold from licking) increases with distal SST stimulation (Δ = 0.46 ± 0.37; $p < 1e{-}5$) and distal PV stimulation (Δ = 0.34 ± 0.26, $p < 1e{-}9$). The magnitude of increase is not significantly different ($p = 0.30$).

D. The reaction time slows with distal SST stimulation (Δ = 0.03 ± 0.07, $p < 0.01$) and distal PV stimulation (Δ = 0.01 ± 0.03 s, $p < 0.01$) with no significant difference across groups ($p = 0.11$).

E. The pupil position is similar between laser and control trials during distal PV stimulation (Δ (laser – control) = –0.17 ± 0.61˚, $p = 0.14$) and SST stimulation (Δ = 0.15 ± 0.50˚, $p = 0.08$).

F. Pupil area (a proxy for arousal, measured as % change from mean) is not different in laser vs control trials during PV stimulation (Δ = –0.61 ± 7.10 %, $p = 0.11$) and SST stimulation (Δ = –1.30 ± 8.15 %, $p = 0.06$).

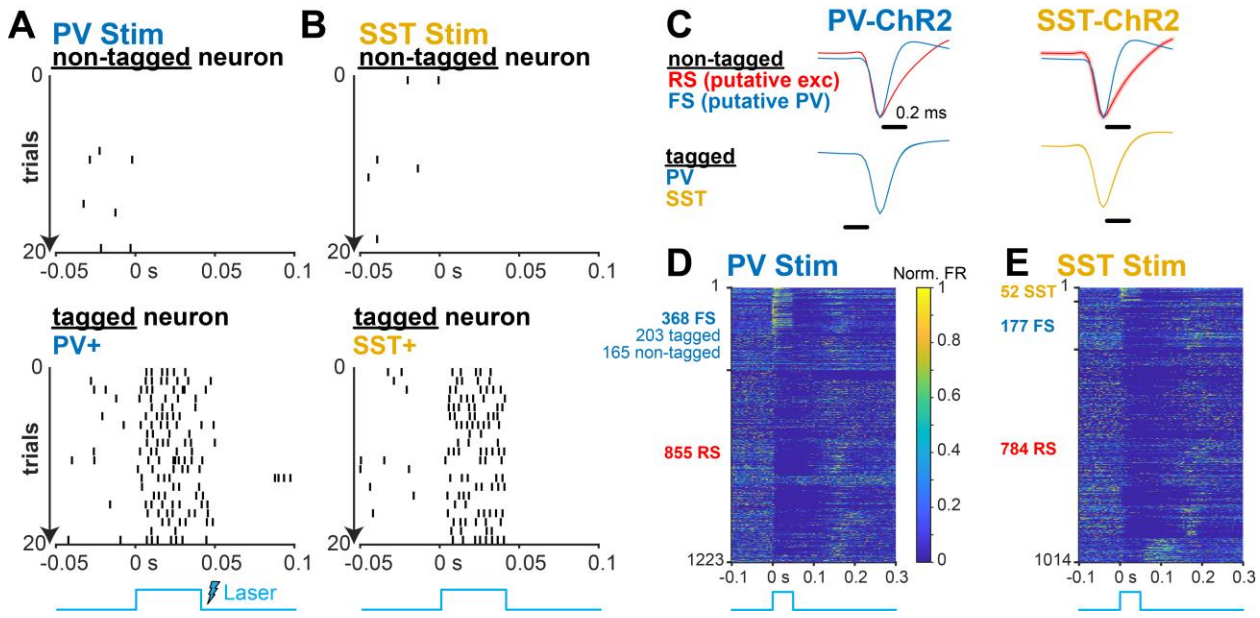

Figure S3. Neuron identification by optotagging and waveform profile.

A. Example non-tagged (top) neuron and opto-tagged (bottom) neuron responses to a brief laser pulse (1.7 mW, 40 ms duration) positioned over the recording site (local stimulation, where recording and stimulation site were the same). In PV-ChR2 mice, neurons were classified as opto-tagged PV neurons if they statistically increased spiking activity rapidly (<10 ms) to a strong laser pulse.

B. Same as A for SST-ChR2 mice. Bottom shows example opto-tagged SST neuron.

C. Non-tagged neurons were classified as fast-spiking (FS) putative PV interneurons or regular-spiking (RS) putative excitatory neurons based on waveform width (FS < 0.57 ms, RS > 0.57 ms). Left, 855 RS neurons, and 368 FS neurons (203 opto-tagged PV neurons; 165 non-tagged) were identified in PV-ChR2 mice. All tagged and non-tagged FS neurons had narrow waveforms and were grouped together for analysis. Right, 785 RS, 177 FS, and 52 opto-tagged SST neurons were identified in SST-ChR2 mice.

D. Responses of all neurons during PV stimulation (normalized to max firing rate). Most FS neurons (both tagged and non-tagged) increased activity to stimulation shortly after onset (203 neurons) while a smaller fraction decreased activity (165 neurons). RS neurons (855 neurons) typically decreased their responses.

E. Same as C for SST stimulation. SST stimulation increases SST (opto-tagged) activity while simultaneously decreasing FS and RS activity.

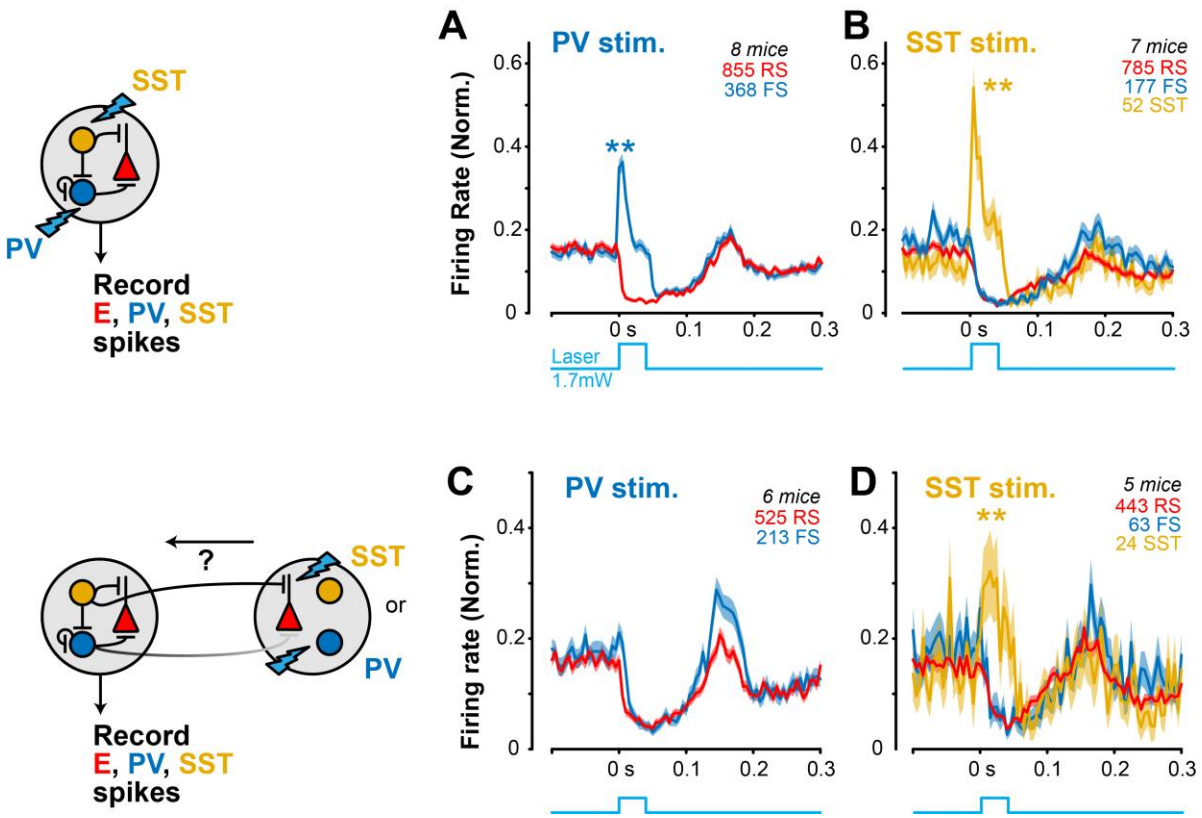

Figure S4. Single unit activity during local and distal PV and SST stimulation

A. Local PV stimulation (brief square pulse, 40 ms duration, 1.7 mW) rapidly increases FS activity (0.14 ± 0.04 MI, mean ± SEM, $p < 0.01$, Wilcoxon signed-rank test) while simultaneously decreasing RS activity (–0.63 ± 0.02 MI, $p <$ 1e–93).

B. Local SST stimulation increases SST activity (0.49 ± 0.08 MI, $p <$ 1e–5), which inhibits FS (–0.45 ± 0.04 MI, $p <$ 1e–14) and RS activity (–0.50 ± 0.02 MI, $p <$ 1e–60).

C. Distal PV stimulation decreases both FS (–0.28 ± 0.04 MI; $p <$ 1e–7, 213 FS neurons) and RS activity (–0.46 ± 0.02 MI; $p <$ 1e–40, 525 RS neurons).

D. Distal SST stimulation decreases RS (–0.33 ± 0.03 MI; $p <$ 1e–17, 443 RS neurons) and FS activity (–0.30 ± 0.07 MI; $p <$ 1e–3, 63 FS neurons), but increases SST activity (0.26 ± 0.09 MI; $p = 0.01$, 24 SST neurons).

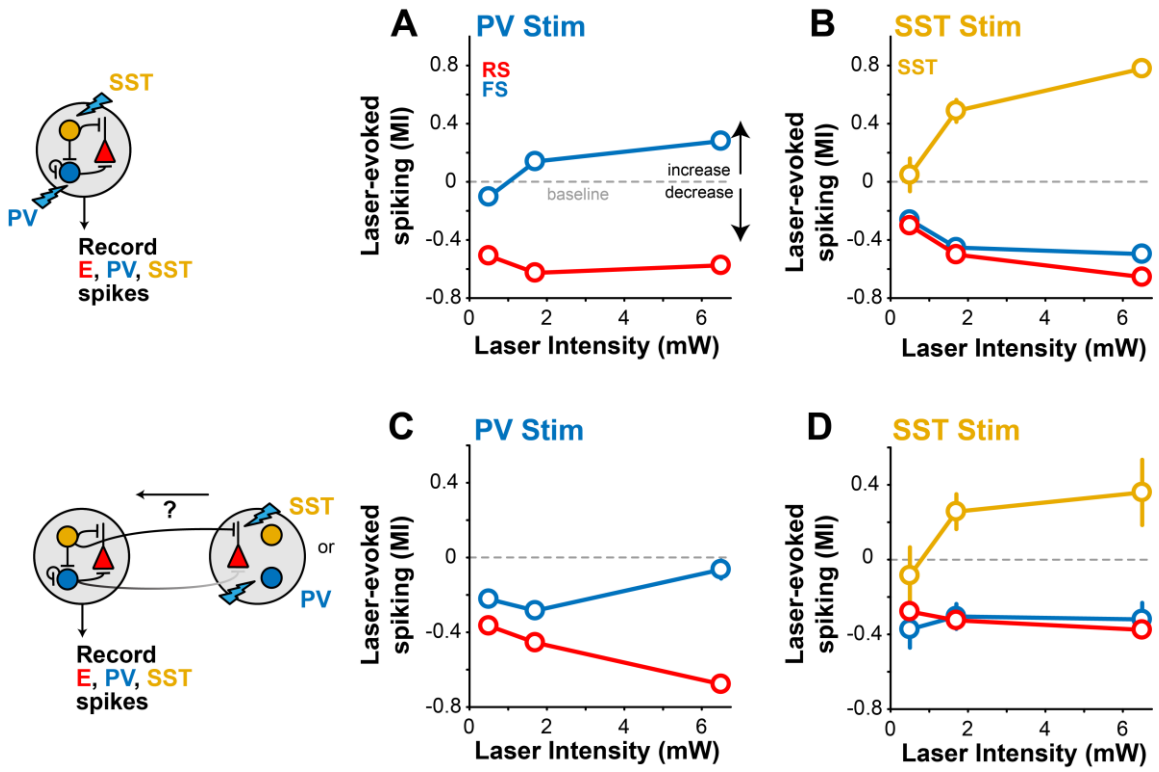

Figure S5. PV or SST stimulation effects across laser intensities.

A. During local PV stimulation, neural activity scales with laser intensity (0.5 – 6.5 mW). FS activity increases and RS activity decreases with stronger laser intensities. Same neurons as in Fig. S4. Moderate power of 1.7mW was used for all main results in study.

B. Same as A for local SST stimulation. SST activity increases with corresponding decreases in FS and RS activity during stronger laser intensities.

C. Same as A for distal PV stimulation. Both FS and RS activity decreased with distal stimulation across laser intensities.

D. Same as B for distal SST stimulation. Despite the laser stimulating a distal cortical site (0.8mm away), SST activity increased across laser intensities while FS and RS activity decreased with distal SST stimulation.

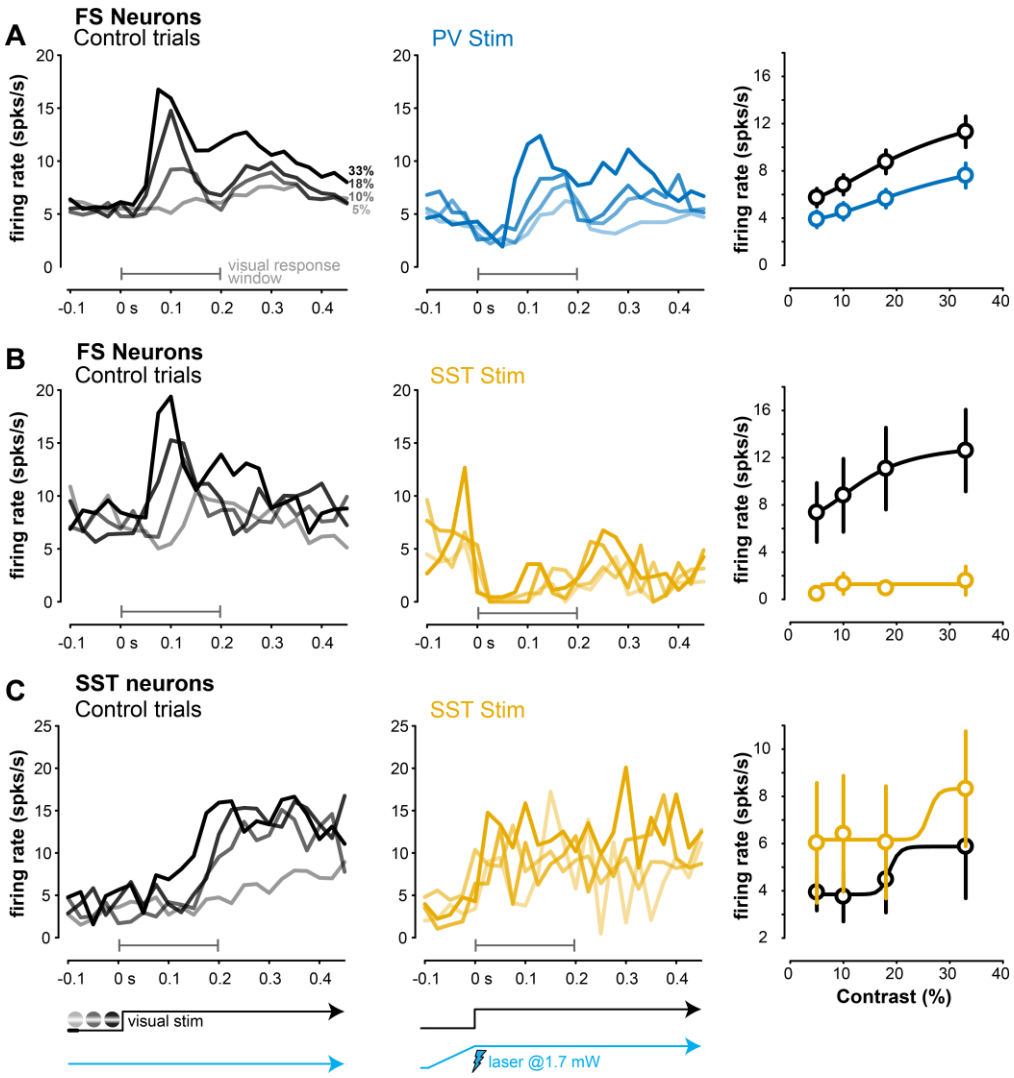

Figure S6. FS and SST activity during distal stimulation and perceptual behavior.

A. FS neuron PSTHs during control (no laser, left) and distal PV stimulation (middle). Distal PV stimulation decreased the slope of FS neurons contrast response function (–0.26 ± 0.51 MI, median ± MAD; p < 1e-4, Wilcoxon signed rank test).

B. Same as for distal SST stimulation. Distal SST stimulation strongly inhibited FS activity across all contrasts. Distal SST stimulation strongly decreased the slope of FS neuron contrast response functions (–0.71 ± 0.47 MI; p < 1e–2). These effects were greater than with distal PV stimulation (p = 0.041, 1-tail Wilcoxon rank-sum test).

C. PSTHs of SST neurons during control (left) and distal SST stimulation (middle). Distal SST stimulation increased SST activity across all contrasts (right; control = 4.91 ± 1.10 sp/s, mean ± SEM; SST stimulation = 8.26 ± 1.71 sp/s; p = 0.06).

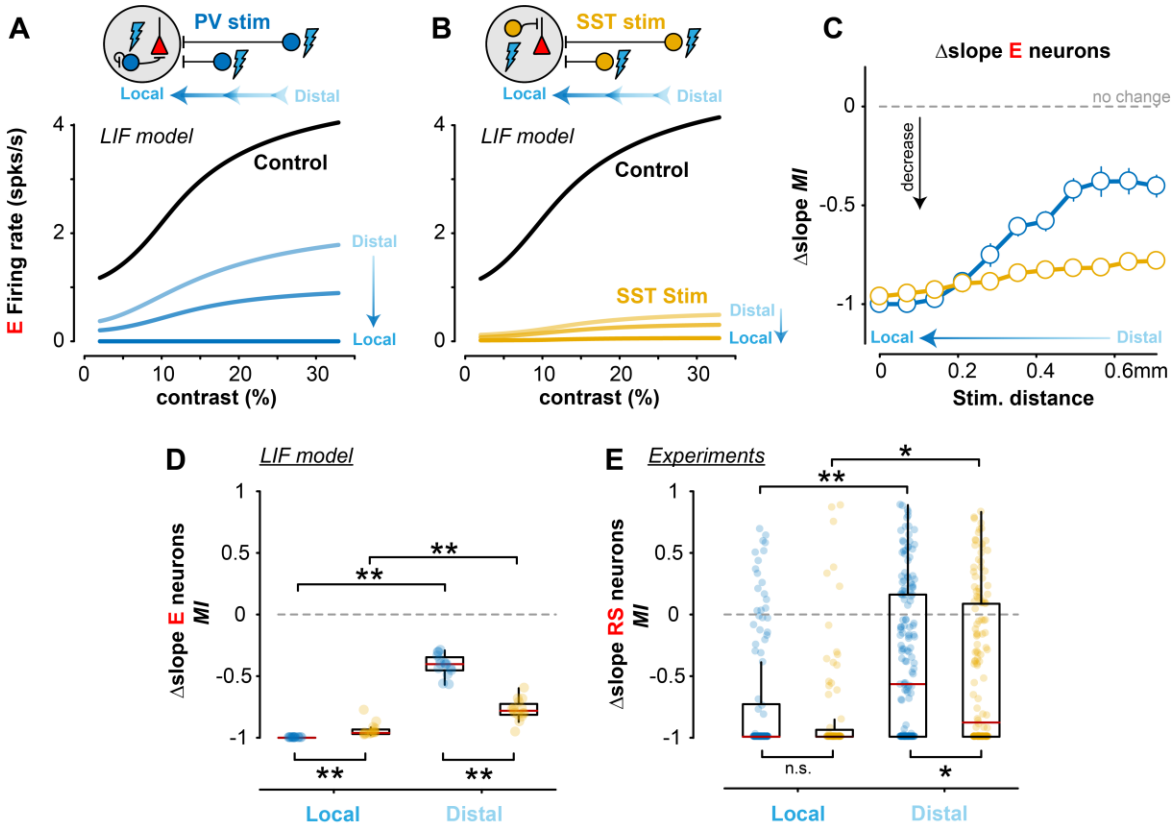

Figure S7. Modulation of contrast sensitivity as a function of stimulation distance

A. Contrast response curves of excitatory neurons in the LIF network model as the site of PV stimulation was applied at 3 varying distances away from the site of visual input. Median ± MAD plotted.

B. Same as A for SST stimulation.

C. Changes in the slope of E neuron contrast sensitivity function (MI, per all other analyses) as a function of stimulation distance. PV stimulation strongly reduced the slope during local stimulation, but the magnitude of effect diminished as the site of stimulation moved farther away. In comparison, SST stimulation exerted strong reductions in slope regardless of stimulation distance. 11 runs per stimulation site. Median ± MAD plotted.

D. Changes in the slope of E neurons during local (stimulation distance = 0 mm) or distal stimulation (stimulation distance = 0.7 mm). Local PV stimulation (–1 ± 0 MI, median ± MAD, Wilcoxon sign-rank test) more strongly decreased the slope than local SST stimulation (–0.96 ± 0.04 MI; p < 1e–6, 1-tail Wilcoxon rank-sum test). The slope change was significantly smaller with distal vs local PV stimulation (p < 1e–6) as was the case with distal vs local SST stimulation (p < 1e–4). However, distal SST stimulation still reduced the slope significantly more (–0.78 ± 0.06 MI) than distal PV stimulation (–0.40 ± 0.06 MI, p < 1e–5).

E. Experimentally recorded RS neuron contrast sensitivity slope changes during perceptual behaviors. Changes in contrast sensitivity slope were not significantly different with local PV stimulation (–1 ± 0.41 MI, 117 RS neurons) vs local SST stimulation (–1 ± 0.32 MI, 75 RS neurons; (p = 0.08). The slope decrease was significantly smaller with distal vs local PV stimulation (p < 1e–7) and with distal vs local SST stimulation (p = 0.021), but importantly, distal SST stimulation decreased the slope (–0.88 ± 0.54 MI, 146 RS neurons) significantly more than distal PV stimulation (–0.57 ± 0.55 MI, 166 RS neurons, p = 0.032), matching the model predictions.

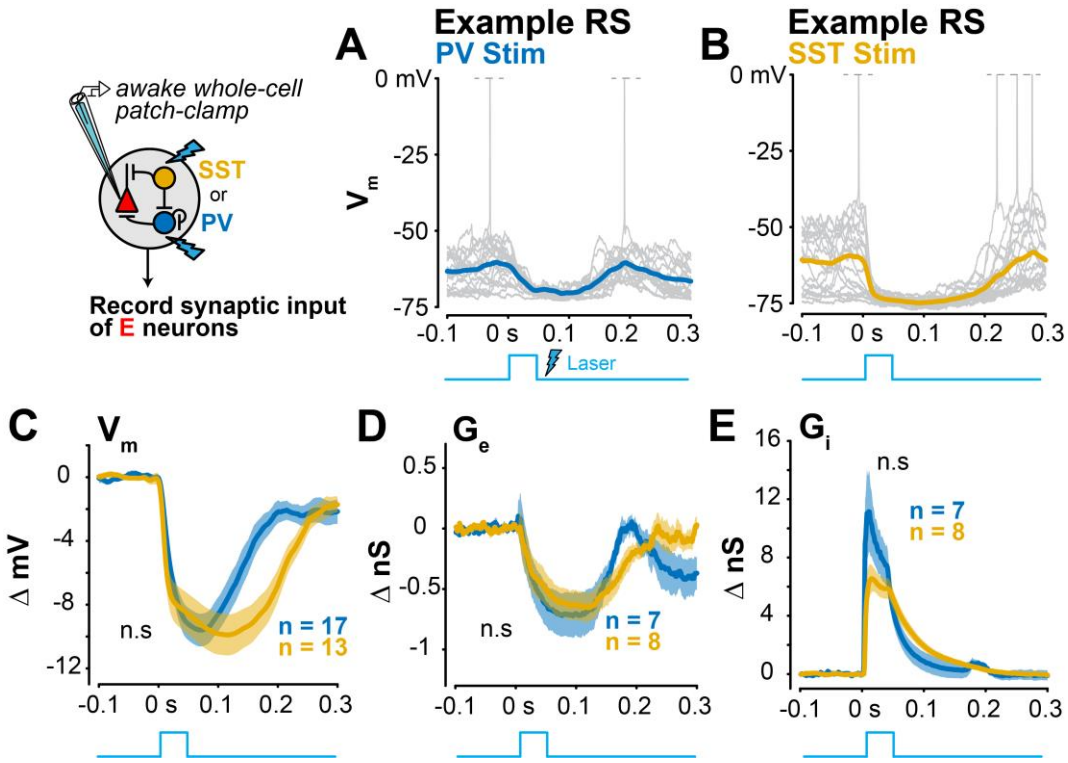

Figure S8. Changes in V_m and conductances in RS neurons during local PV or SST stimulation

A. Example whole-cell current clamp recording in awake V1 RS neuron during local PV stimulation (average across 20 trials plotted). Spikes truncated at 0 mV.

B. Same as A for an example RS neuron during local SST stimulation. Spikes truncated at 0 mV.

C. Hyperpolarization of RS neurons is not significantly different during local PV stimulation (ΔV_m = –6.35 ± 0.79 mV, mean ± SEM, 17 RS neurons) versus local SST stimulation (ΔV_m = –8.45 ± 1.16 mV, 13 neurons; p = 0.08, 1-tail Wilcoxon rank-sum test).

D. Excitatory conductances are reduced with local PV stimulation (ΔG_e = –0.61 ± 0.18 nS, 7 RS neurons) and local SST stimulation (ΔG_e = –0.51 ± 0.13 nS, 8 RS neurons), but they are not significantly different from each other (p = 0.39).

E. Inhibitory conductances increased with local PV stimulation (ΔG_i = 4.85 ± 0.92 nS, 7 RS neurons) and local SST stimulation (ΔG_i = 4.27 ± 0.56 nS, 8 RS neurons), but were not significantly different from one another (p = 0.43).

Table S1. Statistical analysis.

Detailed statistical results used in analysis. Test statistic calculated using z-statistic (or t-statistic when sample size was low, n < 30). Unless otherwise specified, effect size was calculated using r (or Cohen's d for low sample size).

Figure	*Test*	*Test statistic*	*CI (95%)*	*Effect Size*	*DOF*	*p*
Figure 1F - SST group vs null	Wilcoxon signed-rank test	-3.881	[-0.296 -0.125]	-0.514	56	<1e-3
Figure 1F - PV group vs null	Wilcoxon signed-rank test	-1.235	[-0.093 0.0128]	-0.135	83	0.22
Figure 3A - SST group vs null	Wilcoxon signed-rank test	-7.63	[-0.581 -0.384]	-0.631	145	<1e-13
Figure 3A - PV group vs null	Wilcoxon signed-rank test	-7.087	[-0.493 -0.304]	-0.55	165	<1e-11
Figure 3A - SST group vs PV group	1-tail Wilcoxon rank-sum test	-1.853	[-0.220 0.053]	-0.105	310	0.032
Figure 3B - SST group vs PV group	1-tail Wilcoxon rank-sum test	-2.325	[-0.393 -0.018]	-0.1892	149	0.01
Figure 3B - MI = -1: SST group vs PV group	Fisher's exact test	N/A	[0.216 0.924]	0.446 (odds ratio test)	N/A	0.02
Figure 3C: SST group vs null	Hierarchical bootstrapping, percentage MI < 0	-17.930	[-1.380 0.075]	-1.793	99 (bootstrapped)	0.04
Figure 3C: PV group vs null	Hierarchical bootstrapping, percentage MI < 0	-13.792	[-1.306 0.240]	-1.3792	99 (bootstrapped)	0.1
Figure 3E: SST group vs null	Wilcoxon signed-rank test	-6.726	[-0.511 -0.365]	-0.816	67	<1e-10
Figure 3E: PV group vs null	Wilcoxon signed-rank test	-1.54	[-0.164 0.006]	-0.193	63	0.12
Figure 3E: SST group vs PV group	1-tail Wilcoxon rank-sum test	-4.916	[-0.471 -0.247]	-0.428	130	<1e-6
Figure 3F: SST group vs null	Spearman's rank correlation	4.208	[0.221 0.462]	0.347 (ρ)	144	<1e-4
Figure 3F: PV group vs null	Spearman's rank correlation	1.919	[0.026 0.276]	0.154 (ρ)	164	0.048
Figure 5D: SST group vs PV group	1-tail Wilcoxon rank-sum test	-11.932	[-0.421 -0.377]	-0.8437	198	<1e-32

Figure 5E: SST group vs PV group	1-tail Wilcoxon rank-sum test	-12.006	[-0.232 -0.196]	-0.8489	198	<1e-32
Figure 5F: SST group vs PV group	1-tail Wilcoxon rank-sum test	11.544	[0.259 0.320]	0.816	198	<1e-30
Figure 6C: SST group vs PV group	1-tail Wilcoxon rank-sum test	-2.386	[-5.506 -0.902]	-0.436	28	<1e-2
Figure 6D: SST group vs PV group	1-tail Wilcoxon rank-sum test	0.464	[-0.239 0.640]	0.464	13	0.198
Figure 6E: SST group vs PV group	1-tail Wilcoxon rank-sum test	1.539	[0.654 3.182]	1.539	13	<1e-2
Figure S2A: SST group vs null (hit rate)	Wilcoxon signed-rank test	-5.558	[-0.298 -0.173]	-0.736	56	<1e-7
Figure S2A: PV group vs null (hit rate)	Wilcoxon signed-rank test	-7.252	[-0.191 -0.130]	-0.791	83	<1e-13
Figure S2A: SST group vs PV group (hit rate)	1-tail Wilcoxon rank-sum test	1.454	[-0.138 -0.012]	-0.122	139	0.07
Figure S2A: SST group vs null (slope)	Wilcoxon signed-rank test	-2.034	[-0.184 -0.023]	-0.269	56	0.04
Figure S2A: PV group vs null (slope)	Wilcoxon signed-rank test	2.267	[0.004 0.107]	0.247	83	0.02
Figure S2B: SST group vs null	Wilcoxon signed-rank test	-2.336	[-0.089 0.014]	-0.309	56	0.1
Figure S2B: PV group vs null	Wilcoxon signed-rank test	-3.216	[-0.095 -0.009]	-0.351	83	<1e-3
Figure S2B: SST group vs PV group	1-tail Wilcoxon rank-sum test	1.006	[-0.053 0.082]	0.085	139	0.16
Figure S2C: SST group vs null	Wilcoxon signed-rank test	4.596	[0.230 0.467]	0.609	56	<1e-5
Figure S2C: PV group vs null	Wilcoxon signed-rank test	6.052	[0.235 0.392]	0.66	83	<1e-9
Figure S2C: SST group vs PV group	1-tail Wilcoxon rank-sum test	0.531	[-0.101 0.171]	0.045	139	0.3
Figure S2D: SST group vs null	Wilcoxon signed-rank test	2.817	[0.000 0.051]	0.373	56	<1e-2
Figure S2D: PV group vs null	Wilcoxon signed-rank test	2.578	[0.003 0.022]	0.281	83	<1e-2

Figure S2D: SST group vs PV group	1-tail Wilcoxon rank-sum test	1.229	[-0.011 0.037]	0.104	139	0.11
Figure S2E: SST group vs control	1-tail Wilcoxon rank-sum test	1.734	[0.016 0.442]	0.091	356	0.08
Figure S2E: PV group vs control	1-tail Wilcoxon rank-sum test	-1.475	[-0.365 0.216]	-0.077	306	0.14
Figure S2F: SST group vs null	Wilcoxon signed-rank test	-1.867	[-2.830 0.139]	-0.139	179	0.06
Figure S2F: PV group vs null	Wilcoxon signed-rank test	-1.608	[-2.782 -0.187]	-0.118	184	0.11
Figure S4A: FS group vs null	Wilcoxon signed-rank test	2.88	[0.070 0.209]	0.15	367	<1e-2
Figure S4A: RS group vs null	Wilcoxon signed-rank test	-20.547	[-0.663 -0.590]	-0.703	854	<1e-93
Figure S4B: SST group vs null	Wilcoxon signed-rank test	4.545	[0.340 0.636]	0.63	51	<1e-5
Figure S4B: RS group vs null	Wilcoxon signed-rank test	-16.5	[-0.540 -0.462]	-0.589	784	<1e-60
Figure S4B: FS group vs null	Wilcoxon signed-rank test	-7.827	[-0.531 -0.374]	-0.588	176	<1e-14
Figure S4C: FS group vs null	Wilcoxon signed-rank test	-5.656	[-0.360 -0.209]	-0.388	212	<1e-7
Figure S4C: RS group vs null	Wilcoxon signed-rank test	-13.401	[-0.503 -0.408]	-0.585	524	<1e-40
Figure S4D: SST group vs null	Wilcoxon signed-rank test	2.555	[0.074 0.440]	0.522	23	<1e-2
Figure S4D: RS group vs null	Wilcoxon signed-rank test	-8.646	[-0.378 -0.272]	-0.411	442	<1e-17
Figure S4D: FS group vs null	Wilcoxon signed-rank test	-3.423	[-0.435 -0.173]	-0.431	62	<1e-3
Figure S6A: PV group vs null	Wilcoxon signed-rank test	-4.019	[-0.352 -0.136]	-0.376	113	<1e-4
Figure S6B: SST group vs null	Wilcoxon signed-rank test	-2.769	[-0.778 -0.231]	-0.672	16	<1e-2
Figure S6B: SST group vs PV	1-tail Wilcoxon rank-sum test	-1.743	[-0.560 0.038]	-0.152	129	0.041

Figure S6C: SST group vs null	Wilcoxon signed-rank test	-1.254	[-0.646 0.142]	-0.443	7	0.38
Figure S7D: Local SST group vs Local PV group	1-tail Wilcoxon rank-sum test	4.965	[0.033 0.087]	0.907	28	<1e-6
Figure S7D: Local PV group vs Distal PV group	1-tail Wilcoxon rank-sum test	-4.965	[-0.630 -0.544]	-0.907	28	<1e-6
Figure S7D: Local SST group vs Distal SST group	1-tail Wilcoxon rank-sum test	-4.106	[-0.214 -0.113]	-0.75	28	<1e-4
Figure S7D: Distal SST group vs Distal PV group	1-tail Wilcoxon rank-sum test	-4.646	[-0.425 -0.303]	-0.848	28	<1e-5
Figure S7E: Local SST group vs Local PV group	1-tail Wilcoxon rank-sum test	1.387	[-0.208 0.075]	0.1	190	0.08
Figure S7E: Local PV group vs Distal PV group	1-tail Wilcoxon rank-sum test	-5.221	[-0.460 -0.188]	-0.31	281	<1e-7
Figure S7E: Local SST group vs Distal SST group	1-tail Wilcoxon rank-sum test	-2.036	[-0.463 -0.151]	-0.137	219	0.021
Figure S7E: Distal SST group vs Distal PV group	1-tail Wilcoxon rank-sum test	-1.853	[-0.220 0.053]	-0.105	310	0.032
Figure S8C: SST group vs PV Group	1-tail Wilcoxon rank-sum test	-1.423	[-4.760 0.558]	-0.26	28	0.08
Figure S8D: SST group vs PV Group	1-tail Wilcoxon rank-sum test	0.261	[-0.314 0.531]	0.261	13	0.39
Figure S8E: SST group vs PV Group	1-tail Wilcoxon rank-sum test	-0.287	[-2.630 1.471]	-0.287	13	0.43